Analysis of the Bands of the $B^2\Sigma^+$–$X^2\Sigma^+$ Transition in $^{12}C^{16}O^+$ and $^{13}C^{16}O^+$

PRABHAKAR MISRA,[1] DAVID W. FERGUSON, AND K. NARAHARI RAO

Department of Physics, The Ohio State University, Columbus, Ohio 43210

AND

ELMER WILLIAMS, JR.[2] AND C. WELDON MATHEWS

Department of Chemistry, The Ohio State University, Columbus, Ohio 43210

The First Negative bands of $^{12}C^{16}O^+$ and $^{13}C^{16}O^+$, in the spectral region 40 000–46 000 cm^{-1}, have been photographed at a resolution sufficient to resolve the spin-doubled components. These data for $^{12}C^{16}O^+$, along with previously reported data of the same transitions, as well as microwave transitions of $^{12}C^{16}O^+$ in the ground state, have been explicitly included in a least-squares fit to determine the most precise set of molecular constants to date for the $B^2\Sigma^+$ and $X^2\Sigma^+$ states of $^{12}C^{16}O^+$. Furthermore, we report a rotational analysis of the First Negative bands of $^{13}C^{16}O^+$ for the first time. Several molecular constants characterizing $^{13}C^{16}O^+$ in the $B^2\Sigma^+$ and the $X^2\Sigma^+$ states, including spin-doubling parameters, have been determined.

I. INTRODUCTION

The band spectrum of the CO^+ molecule consists of four electronic systems in the region between 11 760 and 55 560 cm^{-1} (that is, between 8500 and 1800 Å). These systems are due to the $B^2\Sigma^+$–$X^2\Sigma^+$ (First Negative), $B^2\Sigma^+$–$A^2\Pi_i$ (Baldet–Johnson), $A^2\Pi_i$–$X^2\Sigma^+$ (Comet–Tail), and $C^2\Delta_r$–$A^2\Pi_i$ (Marchand–D'Incan–Janin) transitions, respectively (*1–4*).

The present study focuses on the First Negative system of $^{12}C^{16}O^+$, which has been examined by several authors (*5–9*) previously. There is a history of contradictory data reported in the literature concerning the spin–rotation coupling constants of the electronic states of $^{12}C^{16}O^+$, as pointed out by Coxon and Foster (*10*) in their study of the $A^2\Pi$–$X^2\Sigma^+$ system. Woods (*6*) obtained the first estimates of γ_v for $X^2\Sigma^+$ in her study of the $B^2\Sigma^+$–$X^2\Sigma^+$ and the $A^2\Pi$–$X^2\Sigma^+$ systems. In a subsequent study of the $B^2\Sigma^+$–$X^2\Sigma^+$ system, Rao (*7*) reported that the values of $|\gamma_v^B - \gamma_v^X|$ were about one-half those reported by Woods. One of the main objectives of the present investigation has been to reexamine the B–X system in $^{12}C^{16}O^+$ in order to resolve the questions regarding differences between the work of Rao and that of Woods, especially in view of recent microwave results.

[1] Present address: Laser Spectroscopy Facility, Department of Chemistry, The Ohio State University, Columbus, OH 43210.

[2] Present address: Rohm and Haas Co., Research Division, 727 Norristown Road, Spring House, PA 19477.

0022-2852/87 $3.00

Fifteen bands for $^{12}C^{16}O^+$ were rotationally analyzed by Rao (*7*) for the B–X system. However, the values reported by Rao for the centrifugal distortion constants for the vibrational levels of both the upper and lower electronic states were only approximations. Based on the resolving power of available instruments in our laboratories, as well as upgraded fitting procedures, a reexamination of the (0, 0), (0, 1) and (0, 2) First Negative bands of $^{12}C^{16}O^+$ has helped determine the most precise set of molecular constants possible with all of the collected data, including Rao's earlier data and more recent microwave observations (*11–13*). The values for $|\gamma_v^B - \gamma_v^X|$ reported earlier by Rao (*7*) are in good agreement with the data obtained from the present examination.

We also report an analysis of the B–X bands of $^{13}C^{16}O^+$. Several parameters characterizing the $^{13}C^{16}O^+$ molecule in the $B^2\Sigma^+$ and the $X^2\Sigma^+$ states are reported for the first time (*9*).

II. EXPERIMENTAL DETAILS

The emission spectra of CO^+ have been recorded on a 3.4-m Jarrell–Ash Ebert spectrograph and on a 10-m Czerny–Turner spectrograph.

For studies made with the Ebert instrument, $^{12}C^{16}O^+$ was formed by using a water-cooled graphite hollow-cathode lamp operating at 600 V and 0.3 A. Argon was initially introduced into the lamp via a needle valve to maintain sufficient pressure to sustain the discharge. Once the discharge stabilized with argon, oxygen was admitted into the discharge tube where it combined with the carbon of the cathode to form $^{12}C^{16}O^+$. The partial pressures of argon and oxygen were regulated so that a steady discharge could be maintained for several hours. Light from the hollow-cathode lamp was focused onto the slit of a predispersion system which served as a narrow band-pass filter for the Ebert spectrograph. The (0, 0) and (0, 2) bands for $^{12}C^{16}O^+$ were recorded in the 25th and 23rd orders, respectively, of a 316 grooves/mm Bausch and Lomb echelle grating blazed at 63.5°. The 3.4-m Ebert spectrograph equipped with the above diffraction grating provided a linear dispersion of about 0.20 Å/mm.

The same bands of $^{12}C^{16}O^+$ were photographed with a Czerny–Turner spectrograph to corroborate the Ebert data and to ascertain the exposure times required for a well-resolved spectrum. For emission studies of $^{12}C^{16}O^+$ made with the Czerny–Turner spectrograph, the discharge was maintained between a hollow stainless-steel cathode and a cylindrical stainless-steel anode. A mixture of helium and carbon dioxide was used to sustain the discharge. To obtain the spectra of $^{13}C^{16}O^+$, carbon dioxide enriched with carbon-13 (~99 at.% pure, supplied by Icon Services of New Jersey) was used in the discharge lamp without further purification. The (0, 0), (0, 1), and (0, 2) bands of the $B^2\Sigma^+$–$X^2\Sigma^+$ system of $^{12}C^{16}O^+$ and $^{13}C^{16}O^+$ were photographed in the 26th, 25th, and 23rd orders, respectively, of a 40 × 20 cm Bausch and Lomb plane grating having 316 grooves/mm at a linear dispersion of about 0.069 Å/mm.

On both instruments the observed resolving power was limited by the temperatures of the source to about 140 000. The spectra were recorded on Kodak SWR and 103a-O plates and on Tri-X and IIaO film with exposure times of about 6 hr with a 30–50 μm spectrograph slit width.

An iron-neon hollow-cathode lamp served as the wavelength calibration source. The iron-neon lines in emission were superimposed along the edges of the CO^+ spectra. The relative positions of the spectral lines were measured with a Grant photoelectric

comparator, which is capable of measuring well-resolved spectral features to abou 0.3 μm.

III. THEORY

For $B^2\Sigma^+$–$X^2\Sigma^+$ transitions, the selection rule for the quantum number N of th total angular momentum apart from spin is $\Delta N = \pm 1$ (*14*). Therefore, the First Negativ bands consist of two series of lines, one series corresponding to $\Delta N = +1$ (the R branch) and the second series to $\Delta N = -1$ (the P branch). The P series consists of th subbranches P_1, P_2, and ${}^pQ_{12}$, while the R series consists of R_1, R_2, and ${}^rQ_{21}$. Th energy level diagram in Fig. 1, for the $B^2\Sigma^+$–$X^2\Sigma^+$ transitions, shows all of the si expected branches. As $\Delta N \neq \Delta J$ for the Q subbranches, ${}^pQ_{12}$ and ${}^rQ_{21}$ are expected t be of exceedingly low intensity and were not seen. Thus, for all practical purposes there is a doublet P branch (P_1, P_2) and a doublet R branch (R_1, R_2). However, th doublet splitting is resolved with clarity only for the higher values of N.

Following Van Vleck (*15*) and Hund (*16*), the rotational energy levels for a ${}^2\Sigma$ state are given by

$$F_1(N) = B_v N(N+1) - D_v N^2(N+1)^2 + \cdots + \tfrac{1}{2}\gamma N \quad (1$$

$$F_2(N) = B_v N(N+1) - D_v N^2(N+1)^2 + \cdots - \tfrac{1}{2}\gamma(N+1), \quad (2$$

where $F_1(N)$ refers to the components with $J = N + \frac{1}{2}$ and $F_2(N)$ to those with $J = N - \frac{1}{2}$. (For more recent Hamiltonians involving Hund's case (b), see Hirota (*17*).) Here B_v and D_v are the effective rotational constants and γ is the spin-splitting constant The above Eqs. (1) and (2) apply both to the $B^2\Sigma^+$ and to the $X^2\Sigma^+$ states. Th wavenumbers of the doublet P branch and the doublet R branch are then given by

$$P_1(N) = \nu_0 + F'_1(N-1) - F''_1(N) \quad (3$$

$$P_2(N) = \nu_0 + F'_2(N-1) - F''_2(N) \quad (4$$

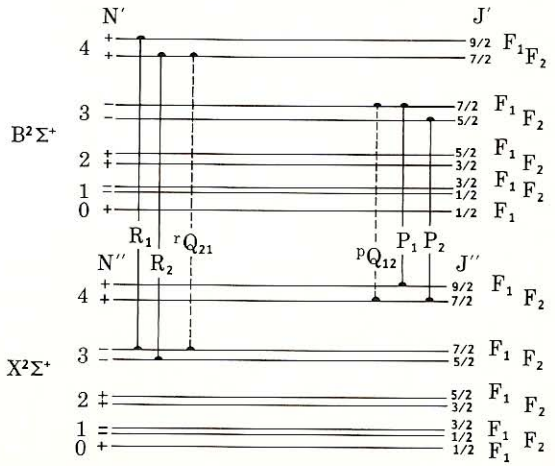

FIG. 1. Energy level diagram for the $B^2\Sigma^+$–$X^2\Sigma^+$ transitions in CO^+.

$$R_1(N) = \nu_0 + F'_1(N+1) - F''_1(N) \tag{5}$$

$$R_2(N) = \nu_0 + F'_2(N+1) - F''_2(N). \tag{6}$$

Here ν_0 is the band origin.

On combining Eqs. (1) and (2) with (3)–(6), the dependence of the observed component splitting on N is shown to be given by

$$\Delta\nu_{(P)} = P_1 - P_2 = (\gamma' - \gamma'')N - \tfrac{1}{2}(\gamma' + \gamma'') \tag{7}$$

$$\Delta\nu_{(R)} = R_1 - R_2 = (\gamma' - \gamma'')N + \tfrac{1}{2}(3\gamma' - \gamma''). \tag{8}$$

Thus, the splitting increases linearly with N, while the magnitude of the splitting depends on the difference between the splitting constants of the upper and lower states. (For the vibrational dependence of γ, see Hirota (*17*).) The N-dependence of the spin-splitting was evident in the experimental wavenumbers of the component doublets. In general, the magnitudes of the splitting constants are quite small, thus indicating that for low N values the splitting is not resolved.

IV. RESULTS AND DISCUSSION

The photographs were calibrated by fitting the iron-neon reference lines (*18*) to a third-degree polynomial (*19*). In the case of $^{12}C^{16}O^+$, the rotational assignments for the (0, 0), (0, 1), and (0, 2) bands were made following the earlier work of Rao (*7*). None of the earlier assignments had to be revised.

The wavenumbers of all spectral lines (except blends) for $^{12}C^{16}O^+$ were used as input data into a nonlinear least-squares fitting program LINFIT developed by Zare *et al.* (*20*) and modified by Griffith (*19*), along with initial estimates of the molecular constants of the $B^2\Sigma^+$ and $X^2\Sigma^+$ states involved in the transitions. Band origins for the (0, 0), (0, 1), and (0, 2) First Negative bands of $^{13}C^{16}O^+$ were estimated initially from the vibrational and rotational isotope shifts (*14*), using $\rho = (\mu/\mu^i)^{1/2} = 0.97778$, where μ is the reduced mass of the $^{12}C^{16}O^+$ molecule and μ^i is that of the $^{13}C^{16}O^+$ molecule. Provisional values of the rotational constants for the $B^2\Sigma^+$ and $X^2\Sigma^+$ states of $^{13}C^{16}O^+$ to be fed as input into LINFIT were obtained using the relation for isotopic molecules (*14*) and the constants for $^{12}C^{16}O^+$.

The vacuum wavenumbers in cm^{-1} for all the spectral lines of the (0, 0) band of $^{12}C^{16}O^+$ recorded with the Ebert spectrograph have been collected in Table I.[3] The vacuum wavenumbers in cm^{-1} of the (0, 2) band of $^{13}C^{16}O^+$ photographed with the Czerny–Turner instrument have been collected in Table II. The components of the doublets have been given wherever they could be measured.

For a given subbranch (e.g., P_1) a plot of the residuals (the difference between the observed and calculated wavenumbers) vs N should be random about zero (i.e., zero slope, with an intercept of zero cm^{-1}). However, as can be seen from the residuals of the P_1 subbranch of the (0, 0) band of $^{12}C^{16}O^+$ in Table I, two systematic patterns

[3] A complete list of assigned transitions and related data is available from the Editor's office of this journal. The data are also available in the Ph.D. dissertations of EW (1985, order number 86-03074) and PM (1986, order number 86-25261) which may be obtained from University Microfilms International, Ann Arbor, MI 48106.

TABLE I

Observed Transitions, ν_{vac} (cm^{-1}), for the (0, 0) Band of $^{12}C^{16}O^+$
(Observed − Calculated Values in Parentheses)

N	P_1	P_2	R_1	R_2
0			45 637.318 (109)	
1	45 629.760 (69)		640.469 (51)	45 640.469 (83)
2	625.474 (78)	45 625.474 (83)	643.299 (38)	643.299 (78)
3	620.798 (63)	620.798 (76)	645.781 (43)	645.781 (92)
4	615.775 (65)	615.775 (88)	647.873 (24)	647.873 (82)
5	610.369 (49)	610.369 (80)	649.603 (01)	649.603 (77)
6	604.618 (53)	604.618 (94)	651.005 (34)	651.005 (110)
7	598.478 (33)	598.478 (83)		
8	591.991 (31)	591.991 (90)		
9	585.126 (16)	585.126 (83)		
10	577.909 (14)	577.909 (91)		
11	570.312 (00)	570.312 (84)		
12	562.357 (-01)	562.357 (84)	651.445 (-56)	651.445 (74)
13	554.045 (-01)	554.045 (94)	650.231 (-64)	650.231 (76)
14	545.346 (-28)	545.346 (84)	648.664 (-53)	648.664 (96)
15	536.311 (-17)	536.311 (104)	646.687 (-79)	646.687 (78)
16	526.869 (-45)	526.869 (85)	644.346 (-96)	644.346 (70)
17	517.113 (-20)	517.113 (119)	641.644(-100)	641.644 (75)
18	506.925 (-59)	506.925 (90)	638.554(-117)	638.554 (68)
19	496.402 (-63)	496.402 (94)	635.104(-118)	635.104 (76)
20	485.479 (-98)	485.479 (68)	631.266(-129)	631.266 (74)
21	474.191(-120)	474.191 (48)	627.118 (-73)	626.954 (-25)
22	462.577(-110)	462.577 (72)	622.457(-150)	622.457(-150)
23	450.568(-120)	450.568 (72)	617.558 (-85)	617.395 (-18)
24	438.207(-100)	438.061 (-53)	612.215 (-84)	612.050 (-01)
25	425.430(-140)	423.369[a]	606.488 (-82)	606.288 (-34)
26	412.257(-180)	412.267(-180)	600.348(-109)	600.163 (-38)
27	398.829(-120)	398.829 (103)	593.898 (-62)	593.615 (-80)
28	384.934(-150)	384.828[a]	587.015 (-62)	586.731 (-71)
29	370.753 (-84)	370.511 (-79)	579.737 (-68)	579.452 (-70)
30	356.203 (-01)	355.903 (-52)	572.087 (-57)	571.783 (-69)
31	341.124 (-83)	340.852 (-90)	564.042 (-51)	463.709 (-82)
32	325.763 (-60)	325.456 (-93)	555.582 (-69)	555.256 (-82)
33	310.001 (-60)	309.684 (-91)	546.774 (-37)	546.409 (-82)
34	293.862 (-50)	293.528 (-90)	537.543 (-35)	537.158 (-91)
35	277.326 (-50)	276.836(-241)	527.922 (-26)	527.500(-110)
36	260.429 (-30)	260.055 (-97)	517.886 (-33)	517.886 (-33)
37	243.120 (-40)	242.731(-110)	507.437 (-53)	507.437 (-53)
38	225.279(-190)	225.103 (-39)	496.402[a]	496.402 (107)
39	207.372 (-20)	206.967 (-87)	485.065[a]	485.065 (145)
40	188.907 (-16)	188.503 (-73)	473.347[a]	473.347 (-54)
41	170.045 (-17)	169.620 (-86)	461.793 (58)	461.289 (-54)
42	150.801 (-01)	150.363 (-80)	449.326 (49)	448.848 (-28)
43	131.167 (01)	130.705 (-79)	436.456 (48)	435.950 (-48)
44	111.128 (16)	110.720 (-01)	423.224 (99)	422.693 (-13)
45	090.692 (24)	090.221 (-55)	409.499 (73)	408.994 (00)
46	069.877 (53)	069.398 (-25)	395.397 (87)	394.883 (00)
47	048.500 (-78)	048.278 (109)	380.871 (96)	380.350 (-21)
48	027.032 (100)	026.514 (04)	365.919 (101)	365.391 (-28)
49	004.958 (84)	004.447 (00)	350.582 (147)	350.004 (-32)
50	44 982.491 (78)	982.019 (43)	334.742 (115)	334.199 (-45)
51	959.690 (148)	959.141 (44)	318.509 (119)	317.962 (53)
52	936.364 (103)	935.900 (94)	301.851 (128)	301.288 (56)
53	912.667 (101)	912.177 (74)	284.758 (137)	284.191 (69)

[a] Lines not used in the least-squares fit.

TABLE I—*Continued*

N	P_1	P_2	R_1	R_2
54			45 267.219 (135)	45 266.654 (78)
55			249.235 (126)	248.644 (52)
56			230.816 (123)	230.248 (81)
57			211.944 (110)	211.362 (63)
58			192.632 (103)	192.093 (109)
59			172.864 (89)	172.271 (50)
60			152.645 (75)	152.041 (34)
61				
62				
63			089.190 (-31)	088.597 (-34)
64			067.092 (-91)	066.488 (-97)
65			044.513(-168)	043.952(-121)
66			021.462(-248)	020.901(-193)
67			44 998.048(-220)	44 998.048(-220)
68			974.748[a]	972.877[a]

occur—one from $N = 1$ to $N = 24$, and the second from $N = 25$ to $N = 53$. The region below $N = 24$ indicates errors from introducing unresolved doublets. The possibility of having misassigned the N values was eliminated by a shift of those values and recalculating the band-by-band fits. Furthermore, it was unnecessary to include higher-order terms in the wavenumber Eqs. (1) and (2), as attempts to do so had little effect on the quality of fit to the observed wavenumbers. The dependence of the spin-splitting constants on N could be eliminated by averaging the wavenumbers of the P subbranch members and then plotting this average vs N. However, when this was done, a linear relationship still did not exist for N ranging between 24 and 35. The origin of this trend appears to be based on two accidental sources of systematic errors: (i) at approximately $N = 15$, the P- and R-branch members begin to overlap, which leads to a systematic shift in the apparent line position, and (ii) at approximately $N = 18$, the (6, 14) band of the A–X transition of CO (2197 Å) is observed (*21*), which also generates a systematic source of error in the apparent line position. Trends described above were evident also in the other subbranch members of the (0, 0) band due to branch crossing, as well as due to the presence of the (1, 1) and (5, 4) bands (located at 2215 and 2223 Å, respectively) of the B–X system of $^{12}C^{16}O^+$ (*22*). The (0, 2) band of $^{12}C^{16}O^+$ also showed similar trends because of branch crossings. The overlapping of the (2, 2) band of the $C^2\Delta_r$–$A^2\Pi_i$ transition of $^{12}C^{16}O^+$ (located at approximately 2439 Å) (*4*) and the overlapping of the (1, 3) band of the $B^2\Sigma^+$–$X^2\Sigma^+$ transition (located at approximately 2446 Å) (*7*) also cause systematic measurement errors. Plots of the residuals for sharp *isolated* lines as a function of N yielded the expected random distribution of points.

For the B–X transitions of $^{12}C^{16}O^+$, results from the band-by-band fits of the present work, the earlier paper of Rao (*7*) and recent microwave transition wavenumbers (*11–13*) were merged. The molecular constants obtained as output from LINFIT served as input to a MERGE computer program, which yielded a final set of molecular constants for the $B^2\Sigma^+$ and the $X^2\Sigma^+$ states. As the MERGE program requires that the bands have at least one vibrational level in common, the (4, 7) band of $^{12}C^{16}O^+$

TABLE II

Observed Transitions, ν_{vac} (cm^{-1}), for the (0, 2) Band of $^{13}C^{16}O^+$
(Observed − Calculated Values in Parentheses)

N	P_1	P_2	R_1	R_2
1	41 392.072 (-17)		41 402.320 (-13)	41 402.320[a]
2	388.869[a]	41 388.869[a]	405.966[a]	405.966[a]
3	383.886 (00)	383.886 (08)	407.722 (-45)	407.722 (-06)
4	379.355 (-14)	379.355 (02)	410.047 (-20)	410.047 (27)
5	374.582 (09)	374.582 (32)	412.063 (-23)	412.063 (30)
6	369.518 (19)	369.518 (48)	413.746 (-80)	413.746 (-20)
7	364.171 (23)	364.171 (60)	415.145[a]	415.145[a]
8	358.528 (10)	358.528 (53)		
9	352.597 (-14)	352.597 (37)		
10	346.403 (-22)	346.403 (36)		
11	339.919 (-41)	339.919 (23)		
12	333.148 (-68)	333.148 (02)		
13	326.147 (-47)	326.147 (31)		
14	318.850 (-42)	318.850 (43)		
15	311.260 (-50)	311.260 (42)		
16	303.385 (-63)	303.385 (35)	415.713 (-41)	415.713 (90)
17	295.239 (-67)	295.239 (39)	414.315 (-71)	414.315 (66)
18	286.936[a]	286.936[a]	412.648 (-84)	412.648 (60)
19	278.100 (-77)	278.100 (43)	410.720 (-70)	410.720 (80)
20	269.119 (-70)	269.119 (56)	408.498 (-63)	408.498 (95)
21	259.832 (-87)	259.832 (46)	405.966 (-77)	405.966 (88)
22			403.150 (-84)	403.150 (88)
23	240.442 (-86)	240.442 (62)	400.037 (-98)	400.037 (81)
24	230.410 (05)	230.410 (159)	396.728 (-15)	396.518 (-40)
25	219.900 (-98)	219.900 (64)	393.066 (07)	392.822 (-44)
26	209.210 (-94)	209.210 (74)	389.074 (-07)	388.869 (-12)
27			384.852 (45)	384.610 (09)
28			380.281 (44)	380.022 (-02)
29			375.394 (24)	375.175[a]
30			370.210 (07)	369.881 (-95)
31			364.811 (74)	364.811[a]
32			358.987 (18)	358.987[a]
33			352.909 (09)	352.909[a]
34			346.531 (05)	346.531[a]
35				339.520[a]
36				332.593[a]
37				
38			318.068 (107)	317.606 (-72)
39			310.142 (97)	309.695 (-60)
40			301.978[a]	301.448 (-72)
41			293.431[a]	292.936 (-32)
42			284.583[a]	284.040 (-61)
43			275.288 (53)	274.830 (-88)
44			265.779 (42)	265.398 (-14)
45			256.024 (106)	255.561 (-26)
46			245.833 (58)	245.342 (-95)
47			235.376 (68)	234.913 (-50)
48			224.492[a]	224.035[a]

[a] Lines not used in the least-squares fit.

as reported by Rao had to be excluded from the fit. The calculated band origins, vibrational quanta and rotational constants obtained as output from MERGE for both states of $^{12}C^{16}O^+$ have been collected in Tables III, IV, and V, respectively. Table VI summarizes the spin-splitting constants of the $B^2\Sigma^+$ and $X^2\Sigma^+$ states for $^{12}C^{16}O^+$.

TABLE III

Origins of the $B^2\Sigma^+$–$X^2\Sigma^+$ System of $^{12}C^{16}O^+$ (cm^{-1})[a]

v'/v"	0	1	2	3	4	5	6
0	45 633.39	43 449.43	41 296.06	39 172.86	37 079.90		
1			42 975.40	40 852.20	38 759.23	36 696.75	
2				42 478.71	40 385.75	38 323.26	36 291.06
3						39 898.76	

[a] The calculated error of the band origins is ± 0.05 cm^{-1}.

In order to minimize the standard deviation of the residuals of the fit, it was necessary to make small corrections to the values of the band origins reported in the earlier work of Rao (*7*). Such adjustments are often necessary, since these reflect the difficulties of absolute wavelength calibration (involving different wavelength regions) as compared to the more precise relative calibrations within the region of a single plate.

The effective rotational constants B_v and D_v are related to the equilibrium constants by

$$B_v = B_e - \alpha_e(v+\tfrac{1}{2}) + \gamma_e(v+\tfrac{1}{2})^2 + \cdots \quad (9)$$

$$D_v = D_e + \beta_e(v+\tfrac{1}{2}) + \delta_e(v+\tfrac{1}{2})^2 + \cdots \quad (10)$$

where α_e, γ_e, β_e, and δ_e are constants. In order to determine values for B_e, D_e, α_e, γ_e, β_e, and δ_e, a weighted polynomial least-squares fitting program was used. The data were fitted to a second-degree polynomial in $(v + \frac{1}{2})$ in order to obtain the desired coefficients. The values for the internuclear distances were derived from the B_e values using

$$B_e = h/(8\pi^2 c\mu r_e^2). \quad (11)$$

The equilibrium constants determined for both states for the $^{12}C^{16}O^+$ transitions are given in Table VII. The dissociation energies of the upper and lower states were estimated from Birge–Sponer plots (*14*).

TABLE IV

Vibrational Quanta[a] of the $B^2\Sigma^+$ and $X^2\Sigma^+$ States of $^{12}C^{16}O^+$

v	$\Delta G'_{v+\frac{1}{2}}$	$\Delta G''_{v+\frac{1}{2}}$
0	1679.333 (51)	2183.971 (38)
1	1626.515 (61)	2153.363 (52)
2	1575.504 (80)	2123.201 (55)
3		2092.961 (60)
4		2062.489 (66)
5		2032.203 (72)

[a] Units are cm^{-1}; the numbers in parentheses represent one standard deviation in the last digits of the constants. The values are based on band origins.

TABLE V

Rotational Constants[a] of the $B^2\Sigma^+$ and $X^2\Sigma^+$ States of $^{12}C^{16}O^+$

v	B_v		D_v ($\times 10^6$)	
	B $^2\Sigma^+$	X $^2\Sigma^+$	B $^2\Sigma^+$	X $^2\Sigma^+$
0	1.784 787 (45)	1.967 465 6 (31)	8.078 (37)	6.354 (38)
1	1.754 66 (10)	1.948 438 8 (43)	8.274 (58)	6.344 (47)
2	1.724 33 (11)	1.929 479 (63)	8.496 (71)	6.437 (41)
3	1.693 93 (20)	1.910 331 (97)	8.63 (13)	6.464 (58)
4		1.891 07 (11)		6.468 (70)
5		1.871 76 (13)		6.466 (84)
6		1.852 55 (17)		6.59 (12)

[a] Units are cm^{-1}; the numbers in parentheses represent one standard deviation in the last digits of the constants.

Plots of the residuals of B_v as obtained from MERGE for $X^2\Sigma^+$ up to $v = 6$ and for $B^2\Sigma^+$ up to $v = 3$ against $(v + \frac{1}{2})$ are shown in Figs. 2 and 3. It is clear that inclusion of recent microwave transitions significantly improves the precision of the B_0'' and B_1'' values, because the uncertainty in the residuals is smaller relative to those of the higher vibrational levels. The residuals plotted in Figs. 2 and 3 are scattered randomly about a line of zero slope with an intercept of zero cm^{-1}, which indicates the correctness of the band-by-band fits.

Inclusion of microwave observations for $^{12}C^{16}O^+$ in the least-squares fits thus allows the precision of all the molecular constants to be improved. The constants reported in this paper are more precise by at least one order of magnitude as compared to those reported in the earlier work of Rao (*7*). The information obtained from a pure rotation spectrum is crucial to determining the most precise set of molecular constants for any observed transition, since the values obtained from optical examinations alone are inherently less precise, but they offer better estimates for the higher-order terms.

In the case of the B–X system of $^{13}C^{16}O^+$, the spin-splitting constant for the $X^2\Sigma^+$ state was fixed at the value $\gamma'' = 0.008\,686(23)$ cm^{-1} cited in the microwave work of Piltch *et al.* (*23*) so as to determine the other rotational constants accurately. The

TABLE VI

Spin-Splitting Constants[a] of the $B^2\Sigma^+$ and $X^2\Sigma^+$ States of $^{12}C^{16}O^+$

v	B $^2\Sigma^+$	X $^2\Sigma^+$
0	0.016 64 (66)	0.009 1051 (89)
1	0.0151 (13)	0.009 048 (12)
2	0.0123 (14)	0.008 46 (25)
3	0.0135 (22)	0.0097 (12)
4		0.0049 (16)
5		0.0063 (17)
6		0.0049 (20)

[a] Units are cm^{-1}; the numbers in parentheses represent one standard deviation in the last digits of the constants.

TABLE VII

Equilibrium Constants[a] for the $B^2\Sigma^+$ and X^2X^+ States of $^{12}C^{16}O^+$

Molecular Constant	B $^2\Sigma^+$	X $^2\Sigma^+$
B_e	1.799 80(11)	1.976 959 5(65)
α_e	0.029 99(20)	0.018 975 (11)
γ_e	$-7(6) \times 10^{-5}$	$-2.47(40) \times 10^{-5}$
r_e	1.168 638(41) Å	1.115 047(27) Å
D_e	$7.964(78) \times 10^{-6}$	$6.327(51) \times 10^{-6}$
β_e	$2(1) \times 10^{-7}$	$3(4) \times 10^{-8}$
δ_e	$0(4) \times 10^{-8}$	$0(7) \times 10^{-9}$
ω_e	1734.48(13)	2214.27(25)
$\omega_e x_e$	27.76(09)	15.20(13)
$\omega_e y_e$	0.301(21)	0.006 6(11)
T_e	45 876.38(33)	0.00
D_o	22 370	63 229

[a] Units are cm^{-1} unless otherwise indicated. The values in parentheses represent one standard deviation in the last digits of the constants.

band origins of the B–X system for $^{13}C^{16}O^+$ are collected in Table VIII. Molecular parameters for the $B^2\Sigma^+$ and the $X^2\Sigma^+$ states of $^{13}C^{16}O^+$ have also been summarized in Table VIII. The absolute values of $|\gamma' - \gamma''|$ obtained for the (0, 1) and (0, 2) bands of $^{13}C^{16}O^+$ are 0.0089(06) cm^{-1} and 0.0069(05) cm^{-1}, respectively.

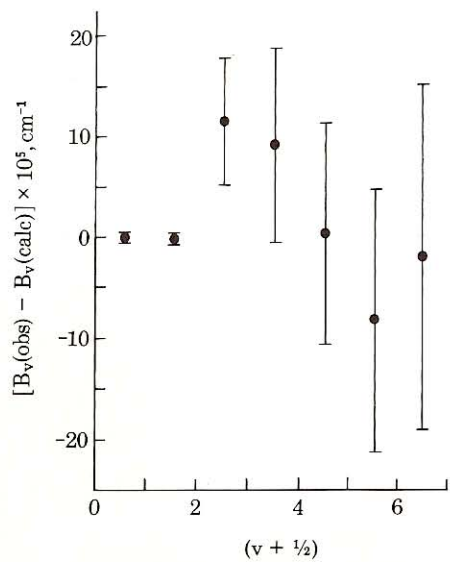

FIG. 2. Plot of $[B_v\ (obs) - B_v\ (calc)]$ vs $(v + \frac{1}{2})$ for the $X^2\Sigma^+$ state of $^{12}C^{16}O^+$.

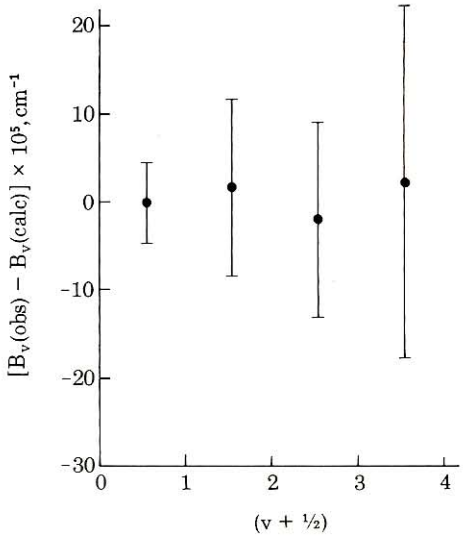

FIG. 3. Plot of $[B_v\ (obs) - B_v\ (calc)]$ vs $(v + \frac{1}{2})$ for the $B^2\Sigma^+$ state of $^{12}C^{16}O^+$.

V. CONCLUSIONS

The results reported here for $^{12}C^{16}O^+$ are in very good agreement with the data in the earlier work of Rao (*7*). The difference $|\gamma' - \gamma''|$ between the spin-splitting constants for each band calculated from the data given in Table VI was compared with the corresponding values reported earlier by Rao (*7*) and by Woods (*6*). This comparison indicates conclusively that $|\gamma_v^B - \gamma_v^X|$ reported by Woods are in error, whereas the values reported earlier by Rao are corroborated by the present study. It is hoped that this paper settles the controversy regarding the spin-splitting constants of the $B^2\Sigma^+$ and the $X^2\Sigma^+$ states of $^{12}C^{16}O^+$ that has existed in the literature over the years.

TABLE VIII

Rotational Constants[a] of the $B^2\Sigma^+$ and $X^2\Sigma^+$ States of $^{13}C^{16}O^+$

Band (v',v")	Origin[b] ν_o	B_v		D_v (x10^5)	
		B $^2\Sigma^+$	X $^2\Sigma^+$	B $^2\Sigma^+$	X $^2\Sigma^+$
(0,0)	45 638.65	1.7115 (22)	1.8868 (22)	0.63 (29)	0.49 (32)
(0,1)	43 502.69	1.7048 (07)	1.8616 (07)	0.68 (09)	0.52 (10)
(0,2)	41 395.78	1.70484(50)	1.8439 (05)	0.639(44)	0.485(48)

[a] Units are cm^{-1}; the numbers in parentheses represent one standard deviation in the last digits of the constants.

[b] The error of the origins is about $\pm 0.05\ cm^{-1}$.

This paper summarizes the most precise set of molecular constants for the $B^2\Sigma^+$ and the $X^2\Sigma^+$ states of $^{12}C^{16}O^+$ reported to date. Results of the analysis of the B–X transitions in $^{13}C^{16}O^+$ document the first observations of spin-doubling in the $^2\Sigma^+$ states and help in the determination of several molecular parameters for this isotopic species.

RECEIVED: January 29, 1987

REFERENCES

1. C. M. BLACKBURN, *Proc. Natl. Acad. Sci.* **11,** 28–34 (1925).
2. M. F. BALDET, *C. R. Acad. Sci. Paris* **178,** 1525–1527 (1924).
3. T. R. MERTON AND R. C. JOHNSON, *Proc. R. Soc. London A* **103,** 383–395 (1923).
4. J. MARCHAND, J. D'INCAN, AND J. JANIN, *Spectrochim. Acta A* **25,** 605–609 (1969).
5. R. F. SCHMID, *Phys. Rev.* **42,** 182–188 (1932).
6. L. H. WOODS, *Phys. Rev.* **63,** 431–432 (1943).
7. K. NARAHARI RAO, *Astrophys. J.* **111,** 50–59 (1950).
8. E. WILLIAMS, JR., Ph.D. dissertation, The Ohio State University, 1985.
9. P. MISRA, Ph.D. dissertation, The Ohio State University, 1986.
10. J. A. COXON AND S. C. FOSTER, *J. Mol. Spectrosc.* **93,** 117–130 (1982).
11. T. A. DIXON AND R. C. WOODS, *Phys. Rev. Lett.* **34,** 61–63 (1975).
12. K. V. L. N. SASTRY, P. HELMINGER, E. HERBST, AND F. C. DE LUCIA, *Astrophys. J.* **250,** L91–L92 (1981).
13. M. BOGEY, C. DEMUYNCK, AND J. L. DESTOMBES, *Mol. Phys.* **46,** 679–681 (1982).
14. G. HERZBERG, "Molecular Spectra and Molecular Structure I: Spectra of Diatomic Molecules," Van Nostrand–Reinhold, New York, 1950.
15. J. H. VAN VLECK, *Phys. Rev.* **33,** 467–506 (1929).
16. F. HUND, *Z. Phys.* **42,** 93–120 (1927).
17. E. HIROTA, "High-Resolution Spectroscopy of Transient Molecules," Springer-Verlag, New York, 1985.
18. H. M. CROSSWHITE, "Fe-Ne Hollow Cathode Tables," Johns Hopkins University, Baltimore, MD, 1965.
19. W. B. GRIFFITH, JR., Ph.D. dissertation, The Ohio State University, 1983.
20. R. N. ZARE, A. L. SCHMELTEKOPF, W. J. HARROP, AND D. L. ALBRITTON, *J. Mol. Spectrosc.* **46,** 37–66 (1973).
21. R. S. ESTEY, *Phys. Rev.* **35,** 309–314 (1930).
22. H. BISKAMP, *Z. Phys.* **86,** 33–41 (1933).
23. N. D. PILTCH, P. G. SZANTO, T. G. ANDERSON, C. S. GUDEMAN, T. A. DIXON, AND R. C. WOODS, *J. Chem. Phys.* **76,** 3385–3388 (1982).